Air Stability of Alkanethiol Self-Assembled Monolayers on Silver and Gold Surfaces

Mark H. Schoenfisch and Jeanne E. Pemberton*

Contribution from the Department of Chemistry, University of Arizona, Tucson, Arizona 85721

Received December 19, 1997

Abstract: Surface Raman spectroscopy, electrochemistry, and X-ray photoelectron spectroscopy have been used to study the effects of air exposure on the stability of self-assembled monolayers (SAMs) formed from alkanethiols on mechanically polished, smooth Ag and Au surfaces. Raman spectra exhibit oxidized sulfur modes after only hours of air exposure. X-ray photoelectron spectroscopy of the S 2p region provides additional evidence for sulfur oxidation. Cyclic voltammetry of $Ru(NH_3)_6^{3+}$ indicates that oxidized alkanethiol SAMs retain blocking characteristics toward electron transfer, even after exposure of the oxidized SAM-surface to a solubilizing solvent. Control experiments suggest ozone as the primary oxidant in ambient laboratory air which causes rapid oxidation of the thiolate moiety. These results have important ramifications for the general use of SAMs in many proposed applications.

Introduction

Organothiol self-assembled monolayers (SAMs) on Ag, Au, Cu, and Pt are of potential utility in a variety of applications including corrosion inhibition and electron-transfer phenomena, as platforms for chemical sensors, and as biomaterials.[1] The ultimate utility of SAMs for these applications will be critically dependent on their stability. Although the structure of SAMs has been thoroughly characterized, their stability in ambient laboratory air has not been adequately characterized and is somewhat controversial based on recent reports[2−4] of rapid oxidation.

Many researchers believe that alkanethiol-SAMs are extraordinarily inert under ambient conditions.[1,5,6] However, organothiol monolayers on Au exposed to air for prolonged periods have been shown to oxidize to sulfinates and sulfonates, indicating their finite stability.[7−10] Once oxidized, aromatic sulfonates have been claimed to subsequently desorb upon aqueous rinsing suggesting weaker surface affinity than the starting SAMs.[11] In addition, it has been established that

oxidized SAMs rapidly exchange with thiols when placed in fresh thiol solutions.[8,10−12]

Li and co-workers were the first to observe sulfonate formation resulting from air exposure of alkanethiol-SAMs [$CH_3(CH_2)_nSH$, n = 3, 5, 7, 8, 11, 15, and 17] adsorbed on Au using laser-desorption Fourier transform mass spectrometry.[7] Sulfonate species were detected from films on Au exposed to the ambient environment for a week. Despite large sulfonate ion signals, the extent of oxidation was not determined. Large sulfonate ion abundances were believed to be the result of a greater ionization efficiency for sulfonates relative to thiolates. No effort was made to study the rate of the oxidation process.

Tarlov and Newman also detected alkanethiol-SAM oxidation on Au after prolonged periods of atmospheric exposure using static secondary ion mass spectrometry (SSIMS).[8] Sulfonate species were detected from SAMs [$CH_3(CH_2)_nSH$, n = 7, 9, 11, 15, and 17] on Au exposed to air for 11 days. However, the rate and extent of oxidation were not reported. Following the hypothesis of Li and co-workers,[7] Tarlov and Newman suggested that the large sulfonate signal was the result of large SSIMS negative ion yields for oxidized sulfur.[8] The sulfonate species formed in this process were shown to be displaced by thiols when reimmersed into thiol solution. No sulfonate species were detected with SSIMS from any SAMs formed in air-saturated thiol/ethanol adsorbate solutions when analyzed immediately following removal from solution. In fact, no evidence for oxidation of SAMs stored in such solutions for periods up to 2 months was observed, suggesting that any sulfonates formed are continuously displaced by thiol molecules.

Horn and co-workers used IR spectroscopy to study the aging of alkanethiol self-assembled monolayers.[9] They found that over a period of ca. 6 months, the relative intensities of the $\nu(C-H)$ bands changed indicating a tilting of alkanethiol molecules away from the surface normal. They ascribed this SAM restructuring to alkanethiol oxidation at the sulfur head-group.

* To whom correspondence should be addressed.

(1) Ulman, A. *Chem. Rev.* **1996**, *96*, 1533−1554.

(2) Wilkins, C. L.; Scott, J. R.; Yao, J.; Fritsch, I.; Everett, W. R. *Abstract #1131*, American Society for Mass Spectrometry, 44th Conference on Mass Spectrometry and Allied Topics, Portland, OR, 1996.

(3) Fritsch, I.; Everett, W. R.; Ha, J., Symposium on Chemically Modified Electrodes: Intelligent Design and Structure, 190th Electrochemical Society Meeting, San Antonio, TX, 1996.

(4) Fritsch, I.; Ehlers, T. J.; Jeter, J.; Scott, J. R.; Wilkins, C. L. Symposium on Spectroscopic Characterization of Thin Films and Interfaces, Federation of Analytical Chemistry and Spectroscopy Societies, 1977.

(5) Laibinis, P. E.; Whitesides, G. M. *J. Am. Chem. Soc.* **1992**, *114*, 9022−9028.

(6) Kumar, A. K.; Biebuyck, H. A.; Whitesides, G. M. *Langmuir* **1994**, *10*, 1498−1511.

(7) Li, Y.; Huang, J.; McIver, Jr., R. T.; Hemminger, J. C. *J. Am. Chem. Soc.* **1992**, *114*, 2428−2432.

(8) Tarlov, M. J.; Newman, J. G. *Langmuir* **1992**, *8*, 1398−1405.

(9) Horn, A. B.; Russell, D. A.; Shorthouse, L. J.; Simpson, T. R. E. *J. Chem. Soc., Faraday Trans.* **1996**, *92*, 4759−4762.

(10) Scott, J. R.; Baker, L. S.; Everett, W. R.; Wilkins, C. L.; Fritsch, I. *Anal. Chem.* **1997**, *69*, 2636−2639.

(11) Garrell, R. L.; Chadwick, J. E.; Severance, D. L. McDonald, N. A.; Myles, D. C. *J. Am. Chem. Soc.* **1995**, *117*, 11563−11571.

(12) Huang, J.; Hemminger, J. C. *J. Am. Chem. Soc.* **1993**, *115*, 3342−3343.

Recently, Scott and co-workers reported the exchange of $CH_3(CH_2)_{11}SH$ SAMs on Au with $CH_3(CH_2)_9SH$ using laser-desorption Fourier transform mass spectrometry (LD-FTMS) in the negative ion mode.[10] Negligible exchange was observed when unoxidized $CH_3(CH_2)_{11}SH$ SAMs were soaked for 30 min in $CH_3(CH_2)_9SH$ solutions. However, quantitative $CH_3(CH_2)_9$-SH exchange was detected for partially oxidized $CH_3(CH_2)_{11}$-SH SAMs with the amount of exchange dependent on the extent of $CH_3(CH_2)_{11}SH$ oxidation. The detection of two thiol populations after soaking was indirectly interpreted in terms of sulfonate formation and displacement. These researchers concluded that the ionization efficiencies of thiolates and sulfonates are approximately equal, suggesting the possibility of extensive SAM oxidation in air, contrary to the reports by Li and co-workers and Tarlov and Newman.

UV-assisted oxidation of alkanethiol SAMs on Au has been more widely reported.[12-18] Photooxidation of SAMs has received considerable attention because of its potential for selective patterning of Au surfaces.[12,13] Rieley and co-workers used near edge extended X-ray absorption fine structure and ultraviolet photoemission spectroscopy to study the photooxidation of $CH_3(CH_2)_7SH$ SAMs on Au (111).[15] They theorized that incident UV radiation absorbed by the Au surface produces O_2^- which can subsequently oxidize adsorbed thiolate species to the sulfonates. Extensive sulfonate formation was observed in regions of the surface exposed to UV light.

Hutt and Leggett studied the effects of UV irradiation of methyl terminated alkanethiols [$CH_3(CH_2)_nSH$, $n = 2, 5, 7, 9, 11, 15$, and 17] on Au using XPS.[18] They also observed significant thiolate oxidation to sulfonate species by "active" O_2 species as a result of UV exposure. The rate of photooxidation was found to vary significantly with alkyl chain length; short-chain length SAMs oxidize much faster than long-chain SAMs.

Lewis, Tarlov, and Carron studied the photooxidation process of alkanethiol SAMs [$CH_3(CH_2)_nSH$, $n = 5, 9$, and 17] on electrochemically roughened Ag using surface-enhanced Raman scattering (SERS) and concluded that UV irradiation in air photochemically induces C–S bond scission.[16] The alkyl chain fragments subsequently desorb so that the surface-bound sulfur is exposed to the air and is oxidized. Similar behavior was observed for benzenethiolate and tetradecanethiolate monolayers on Au by Garrell and co-workers using SERS and a quartz crystal resonator.[19] The final oxidation product, adsorbed SO_4^{2-}, easily rinsed away with water. However, some uncertainty regarding the effects of surface morphology on sulfate-Ag affinity must be noted, because these two SERS studies were performed on SAMs on roughened surfaces.

Despite the interest in using SAMs for a variety of applications, few studies have thoroughly investigated alkanethiol oxidation in the ambient laboratory environment with spectroscopic techniques. The air stability of SAMs may be of considerable importance to the photopatterning community because of the need to selectively control oxidation. Thus, the goal of the studies presented here is to obtain a better understanding of SAM stability in ambient laboratory air without UV irradiation or light exposure. Surface Raman spectroscopy, X-ray photoelectron spectroscopy (XPS), and cyclic voltammetry are utilized to study the effects of air exposure on the structure of SAMs formed from three alkanethiols ($CH_3(CH_2)_n$-SH, $n = 2, 11$, and 17) on mechanically polished, smooth, polycrystalline Ag and Au surfaces. The combination of these characterization tools provides a more detailed picture of the effects of air exposure on SAM structure and bonding than has previously been elucidated.

Experimental Section

Chemicals. Propanethiol (99%), dodecanethiol (98%), octadecanethiol (98%), and thiophenol (99+%) were purchased from Aldrich and either used as received or purified by distillation. Ethanol (absolute) was purchased from Quantum Chemical Corp. Bulk polycrystalline Ag (99.999%) and Au (99.999%) were purchased from Johnson Matthey. Distilled, deionized water was purified with a reverse osmosis (RO 10 Plus) system from Millipore Corp. (Bedford, MA) and then purified further with a Milli-Q UV Plus system (Millipore). N_2 (99.995%), O_2 (99.7%), and compressed air (medical grade = 19–23% O_2 [99.7% purity], balance N_2 [99.995% purity]) were obtained from U.S. Airweld (Tucson, AZ). Hexane (99.9%) was purchased from Fischer. KCl (99.7%) was purchased from Mallinckrodt. Hexaammineruthenium(III) chloride (Ru 32%) was purchased from Johnson Matthey. All chemicals were used as received unless noted.

Surface Preparation. Polycrystalline Ag and Au surfaces (geometric surface area ca. 0.80 cm² for Raman and XPS, ca. (7–8) × 10^{-3} cm² for cyclic voltammetry) were cleaned either by sanding on 1500 grit silicon carbide sandpaper or Piranha solution immersion, respectively. (*Caution! Piranha solution is a very strong oxidant and can spontaneously detonate upon contact with organic material!*) The surfaces were then mechanically polished with successively finer grades of agglomerated alumina down to 0.05 μm on a padded lapping wheel (Ecomet I, Buehler Ltd.). Subsequently, these surfaces were rinsed with water and ethanol. A Bransonic 220 ultrasonic cleaner was employed for removal of residual alumina trapped at the surface. Au surfaces were electrochemically polished by at least 10 cycles from −0.2 V to +1.2 V at 100 mV/s in 1.0 M H_2SO_4. In addition, Au surfaces were slightly electrochemically roughened by applying three linear potential sweep oxidation reduction cycles (ORCs) in 0.1 M KCl between −0.2 V and +1.2 V at a sweep rate of 100 mV/s to generate slight surface enhancement and higher signal levels. This protocol results in ca. 10 mC/cm² of anodic charge passed per sweep.

SAM Formation. Surfaces were first rinsed with anhydrous ethanol prior to immersion into a 10 mM thiol solution. Solutions of organothiols in ethanol were prepared using a freshly opened bottle of anhydrous ethanol in a glovebag purged by N_2. Film formation times on Au surfaces were 3 h for $CH_3(CH_2)_2SH$, 24 h for $CH_3(CH_2)_{11}SH$, and 24 h for $CH_3(CH_2)_{17}SH$.

For Ag surfaces, an electrochemical cleaning step was carried out after SAM film formation to further clean the Ag surface. As has been shown previously in this laboratory,[20] carbon contamination can be present in these films upon their initial formation as a result of residual carbon from mechanical polishing. Negative potentials beyond those of alkanethiol reductive desorption have been shown to remove these carbonaceous impurities as well as the alkanethiol molecules. An additional immersion period (identical in time to the original) after such treatment is used to form a complete, well-annealed film. As ascertained by Raman spectroscopy and cyclic voltammetry, films with superior order and cleanliness are formed by this protocol.[21]

Sample Handling. Rigorous precautions were taken to ensure a dark, O_2-free SAM formation environment for these experiments by working in a N_2-filled glovebag. Air exposure of the alkanethiol solution during film formation was further prevented by a steady blanket

(13) Tarlov, M. J.; Burgess, Jr., D. R. F.; Gillen, G. *J. Am. Chem. Soc.* **1993**, *115*, 5305–5306.

(14) Huang, J.; Dahlgren, D. A.; Hemminger, J. C. *Langmuir* **1994**, *10*, 626–628.

(15) Rieley, H.; Price, N. J.; White, R. G.; Blyth, R. I. R.; Robinson, A. B. *Surf. Sci.* **1995**, *331–333*, 189–195.

(16) Lewis, M.; Tarlov, M.; Carron, K. *J. Am. Chem. Soc.* **1995**, *117*, 9574–9575.

(17) Behm, J. M.; Lykke, K. R.; Pellin, M. J.; Hemminger, J. C. *Langmuir* **1996**, *12*, 2121–2124.

(18) Hutt, D. A.; Leggett, G. L. *J. Phys. Chem.* **1996**, *100*, 6657–6662.

(19) R. L. Garrell, private communication.

(20) Taylor, C. E.; Garvey, S. D.; Pemberton, J. E. *Anal. Chem.* **1996**, *68*, 2401–2408.

(21) Schoenfisch, M. H.; Ross, A. M.; Pemberton, J. E., to be submitted.

of N_2 in the immersion vessel. After emersion from the organothiol solution, surfaces were rinsed with 100% ethanol, allowed to dry in the N_2 environment of the glovebag, and transferred to a N_2-purged spectrochemical cell while in the N_2-filled glovebag. The electrochemical cleaning protocol described above for Ag was also carried out in the glovebag. Thus, prior to the start of each experiment, the *SAM-modified surfaces were never exposed to the ambient atmosphere*.

Once films were formed, the surfaces were exposed to either the ambient laboratory environment, N_2, O_2, compressed air, or O_3 in either the spectrochemical cell or a glovebag purged continuously with the gas of interest. All experiments were carried out in complete darkness.

O_3 was prepared using a Boekel Model 135500 dry process cleaner (Boekel Industries, Inc.) inside a glovebag purged with compressed air. A low-pressure Mercury grid lamp enclosed in a reaction chamber generates an environment rich in O_3 which can be flushed into the glovebag by a stream of N_2 or compressed air. *Caution: This procedure should be performed under a hood, since ozone is toxic*. The SAM-modified Ag and Au surfaces were not exposed to UV light during O_3 production.

Raman Spectroscopy. Raman spectroscopy of SAM-modified Au and Ag surfaces was performed on a system described previously.[20] Spectra for SAM-modified surfaces were collected with 514.5 nm excitation from a Coherent Innova 90-5 Ar$^+$ laser for Ag and 720 nm excitation from an Ar$^+$ laser-pumped Lexel model 479 Ti-sapphire laser for Au. Laser powers of 150 mW at the sample were used for both excitation wavelengths. Integration times were 60 s co-added five times for a total of 5 min for SAMs on Ag and 10 s co-added 90 times for a total of 15 min for SAMs on Au. Detection of the Raman scattered radiation was accomplished using either a 512 × 512 thinned, back-illuminated TK512 CCD-based system from Princeton Instruments (Ag) or a 512 × 512 frontside-illuminated Photometrics PM512 CCD system (Au), both cooled to −110 °C.

Cyclic Voltammetry. Cyclic voltammetry of SAM-modified surfaces was performed with a Bioanalytical Systems 100W electrochemical workstation in a three-electrode configuration. A Pt wire was used as the counter electrode. Potentials were measured and are reported versus a Ag/AgCl (saturated KCl) reference electrode.

XPS. XPS measurements were made on modified-Ag and Au surfaces using a Vacuum Generators ESCALAB MKII electron spectrometer equipped with a concentric hemispherical analyzer and a channel electron multiplier detector. The base pressure in the analyzer chamber was ca. 5×10^{-9} Torr. X-rays from the Al K$_\infty$ line at 1486.6 eV at a flux of 200 W were used for excitation. Electrons were collected in the constant analyzer energy (CAE) mode with a pass energy of 50 keV. Integration times were 0.25 s co-added four times for a total of 1.0 s at an interval of 0.1 eV. The areas under the unsmoothed S 2p peaks were measured using a Shirley background correction method.[22] Spectra shown here have been smoothed by a five-point Savitzky-Golay function. Relative peak area ratios were calculated using previously published photoionization cross-sections[23] and accounting for the transmission properties of the analyzer.

Mass Spectrometry. Residual gas analysis of an aliquot of ambient laboratory air was performed with a Balzers Prisma Model QMS 200 quadrupole-based mass spectrometer housed in an UHV chamber with a base pressure of ca. 2×10^{-10} Torr.

Results and Discussion

SAMs on Ag. Raman Spectroscopy. Surface Raman spectra were collected in a controlled-atmosphere spectrochemical cell in which the surface is continually rotated.[21] This cell has two advantages for studying surface oxidation: a controlled environment can be maintained by purging the cell with the gas of interest, and degradation of the sample by extensive laser exposure is prevented by continuous surface rotation.

Raman spectra in the $\nu(C-S)$, $\nu(C-C)$, and $\delta(C-H)$ region (ca. 600−1700 cm^{-1}) from CH$_3$(CH$_2$)$_2$SH, CH$_3$(CH$_2$)$_{11}$SH, and CH$_3$(CH$_2$)$_{17}$SH SAMs on Ag before air exposure are shown in

Figure 1 (parts a, e, and i, respectively). The $\nu(C-S)_G$ and $\nu(C-S)_T$ modes for alkanethiols at ca. 630 and 705 cm^{-1}, respectively, indicate well-ordered SAMs near the thiol head-group.[24,25] No evidence of oxidation is apparent.

A weak $\nu(C-S)_G$ mode is visible in all spectra, presumably due to slight disorder introduced by metal grain and alkanethiol domain boundaries. In previous work from this laboratory,[25] it has been noted that slightly greater disorder is observed in the vicinity of the headgroup with intentionally roughed surfaces. Alkanethiol SAMs apparently accommodate surface roughness with disorder near the headgroup, resulting in the observed ν-(C−S)$_G$ intensity in all SAM spectra.

Further evidence for the quality of these SAMs comes from electrochemical capacitance measurements. Capacitance values of 9.1 ± 6.5, 5.1 ± 2.6, and 4.2 ± 1.9 μF/cm^2 are measured for CH$_3$(CH$_2$)$_2$SH, CH$_3$(CH$_2$)$_{11}$SH, and CH$_3$(CH$_2$)$_{17}$SH films on Ag, respectively. These values are similar to those previously reported for ordered SAMs on freshly evaporated Au surfaces.[26−28] (Capacitance values for SAMs on Ag have not been published.) Thus, on the basis of these measurements and the spectra shown in Figure 1 (parts a, e, and i), we conclude that these SAMs on Ag are well-ordered and show no evidence of oxidation.

SAMs formed in air-saturated alkanethiol solutions and emersed into the ambient environment are also free of oxidation similar to the previous results of Tarlov and Newman.[8] This observation suggests that efforts to completely exclude air during immersion and sample transfer may be unimportant. Nonetheless, all SAMs used here were formed in alkanethiol solutions from which air was excluded and transferred to the spectrochemical cell or XPS fast-entry port in a pure N_2 environment.

SAM-modified Ag surfaces were exposed to the ambient laboratory air in the dark by removing the N_2 purge. As shown by the spectra in Figure 1 (parts b, f, and j), significant changes indicative of film oxidation are observed after only 2 h. The $\nu(C-S)_G$ band at 630 cm^{-1} broadens and shifts to lower frequencies due to an oxidation band that grows in at ca. 615 cm^{-1}. In addition, a peak at 975 cm^{-1} appears, and a broad background develops beneath the peaks in the 900−1200 cm^{-1} region. These spectral changes clearly indicate sulfur headgroup oxidation to the corresponding alkyl sulfonates based on previous reports of SAM oxidation after UV exposure.[16] Abbreviated vibrational assignments for oxidized sulfur species are given in Table 1.[29]

With increasing air exposure, the relative intensities of the oxidation modes increase and discrete bands resolve, suggesting progressive oxidation. These changes are clearly seen in the

(22) Shirley, D. A. *Phys. Rev.* **1972**, *B5*, 4709−4714.

(23) Schofield, J. *J. Electron Spectrosc. Relat. Phenom.* **1976**, *8*, 129−137.

(24) Bryant, M. A.; Pemberton, J. E. *J. Am. Chem. Soc.* **1991**, *113*, 3629−3637.

(25) Bryant, M. A.; Pemberton, J. E. *J. Am. Chem. Soc.* **1991**, *113*, 8284−8293.

(26) Finklea, H. O.; Avery, S.; Lynch, M.; Furtsch, T. *Langmuir* **1987**, *3*, 409−413.

(27) Porter, M. D.; Bright, T. B.; Allara, D. L.; Chidsey, C. E. D. *J. Am. Chem. Soc.* **1987**, *109*, 3559−3568.

(28) Walczak, M. M.; Chung, C.; Stole, S. M.; Widrig, C. A.; Porter, M. D. *J. Am. Chem. Soc.* **1991**, *113*, 2370−2378.

(29) In an effort to correlate oxidation bands in the surface Raman spectra of alkanethiol SAMs to sulfates, spectra of solid Na$_2$SO$_4$ and NaHSO$_4$ were collected. Several bands in the spectra of these sulfate salts are clearly observed in the surface Raman spectra of SAMs on Ag, specifically the δ(SO$_4{}^{2-}$) at 615 cm^{-1}, the ν_s(SO$_4{}^{2-}$) at 875 cm^{-1}, the ν_{as}(SO$_4{}^{2-}$) at 1040, and the ν_s(SO$_2$) at 1147 cm^{-1}. (See, for example, Nakamoto, K. *Infrared and Raman Spectra of Inorganic and Coordination Compounds*, 4th ed.; John Wiley & Sons: New York, 1986; pp 248−251.) However, the oxidized SAM peaks at 975, 1195, and 1395 cm^{-1} are not accounted for in the sulfate salt Raman spectra, suggesting sulfur headgroup oxidation to multiple oxidized species possibly including sulfonates, sulfinites, sulfites, and sulfates.[11]

Table 1. Raman Spectral Assignments for Sulfur Oxidation Modes[11,16,29]

mode	freq (cm^{-1})
$\delta(SO_4^{2-}$ or $R{-}OSO_3^{2-})$	615
$\nu_s(SO_4^{2-}$ or $R{-}OSO_3^{2-})$	975
$\nu_s(R{-}SO_3^-)$	1034
	1127
$\nu_{as}(SO_4^{2-}$ or $R{-}OSO_3^{2-})$	1040
$\nu_a(R{-}SO_3^-)$	1195

spectra by comparing the spectra in Figure 1. *These observations demonstrate that well-ordered alkanethiol-SAMs on Ag oxidize after only hours of air exposure without UV irradiation.*

Oxidation proceeds most rapidly and completely for $CH_3(CH_2)_2SH$ based on the appearance and intensity of the oxidation bands at 615, 975, 1034, 1040, 1127, and 1195 cm^{-1} after 2 h of air exposure. The longer-chain alkanethiols ($CH_3(CH_2)_{11}SH$ and $CH_3(CH_2)_{17}SH$) do not oxidize as quickly, presumably due to increased van der Waals interactions which slow penetration of the oxidant. Similar conclusions about the rates of UV-induced oxidation as a function of chain length were made by Laibinis and Whitesides,[5] Lewis and co-workers,[16] and Hutt and Legett.[18]

At first glance, the intensity ratio of the $\nu(C{-}S)_G$ to $\nu(C{-}S)_T$ modes appears to increase with oxidation indicating disorder of the alkane chain near the headgroup. Although this behavior might be expected, since the monolayer near the headgroup must reorganize to accommodate sulfur oxidation, a $\delta(R{-}OSO_3^{2-})$ mode at 615 cm^{-1} which overlaps the $\nu(C{-}S)_G$ makes this conclusion tenuous. Curve fitting of spectra in the $\nu(C{-}S)$ region suggests that as oxidation progresses, the alkyl chain in the vicinity of the headgroup indeed disorders. The $\nu(C{-}S)_G/\nu(C{-}S)_T$ peak area ratio for each chain length increases with air exposure time and oxidation.

The amount of disordering that accompanies oxidation is most pronounced for $CH_3(CH_2)_2SH$. The $\nu(C{-}S)_G/\nu(C{-}S)_T$ peak area ratio increases from 0.6 to 2.3 after exposure to air for 18 h. In contrast, the $\nu(C{-}S)_G/\nu(C{-}S)_T$ peak area ratios for $CH_3(CH_2)_{11}SH$ and $CH_3(CH_2)_{17}SH$ SAMs increase from 0.1 to 0.4 and 0.1 to 0.3, respectively, after a similar air exposure time. These results are consistent with slower oxidation and less disordering of the longer SAMs due to impeded penetration of the oxidant species.

Surface Raman spectra from alkanethiol SAMs on Ag exposed to air in the dark for 15 days are shown in Figure 2. All three monolayers are extremely oxidized. The broad feature at ca. 975 cm^{-1} suggests that the predominant oxidized species are derivatives of sulfate and sulfonate. Significantly, the presence of $\nu(C{-}S)_T$ and $\nu(C{-}C)_T$ peaks at 706 and 1026 cm^{-1} in Figure 2a, 718, 1030, and 1110 cm^{-1} in Figure 2b, and 723, 1058, 1101, and 1125 cm^{-1} in Figure 2c suggest that the alkane portions of these molecules are still present at the interface and somewhat ordered. Tarlov and co-workers reported that they did not observe any oxidation peaks in the Raman spectra of UV-exposed SAMs until the monolayer bands first decreased significantly.[16] They further suggested that oxidation of the sulfur headgroup requires removal of the hydrocarbon chains to allow easier oxygen access. In contrast, no such intensity decrease prior to oxidation is observed in these spectra, suggesting that significant oxidation occurs without hydrocarbon chain removal, perhaps by penetration of the oxidant through SAM defect sites.

Effect of Application of Negative Potential. Selective removal of oxidized short chain alkanethiol species on Ag can be achieved by application of negative potentials in 0.1 M NaF. An example of this behavior is shown in Figure 3 for $CH_3(CH_2)_2SH$ films. The presence of sulfonate peaks after 20 h of air exposure indicates extensive oxidation. Exposure of this SAM to a 0.1 M NaF solution for ca. 5 min at -0.05 V results in few spectral changes (Figure 3c), suggesting that the sulfonate species remain bound at the interface. However, extensive spectral changes are observed at -1.1 V (Figure 3d). The disappearance of the majority of bands due to the oxidized species suggests that they are removed from the surface, presumably due to repulsion at these negatively charged surfaces. Bands due to the native alkanethiol species are still observed, however, confirming that the oxidized species are less tightly bound to Ag than the thiolates.[8,18] The $\nu(C{-}S)_T$ and $\nu(C{-}C)_T$ bands at ca. 710 and 1030 cm^{-1} are intense relative to the $\nu(C{-}S)_G$ band at 630 cm^{-1} indicating that the native alkanethiols remain fairly ordered. Such order is likely responsible for the significant activation (-1.1 V) required for removal of the oxidized forms of $CH_3(CH_2)_2SH$ incorporated into such films.

In contrast, no significant spectral changes are observed at negative potentials of up to -2.0 V for air-oxidized $CH_3(CH_2)_{11}SH$ and $CH_3(CH_2)_{17}SH$ SAMs on Ag. These results suggest that the van der Waals interactions of longer chain length SAMs prevent the removal of the oxidized species from the surface. This observation contradicts previous reports of the instability of oxidized SAMs toward disruptive perturbations such as exposure to solubilizing solvents.[11,13]

Cyclic Voltammetry. Previous reports[8,10,11,30] indicate rapid desorption of oxidized sulfur species when placed in a solubilizing solvent. To ascertain the extent to which such loss occurs from these oxidized SAMs, cyclic voltammetry of $Ru(NH_3)_6^{3+}$ was used to estimate the amount of exposed Ag surface before and after oxidation of the SAM. These results are interpreted assuming that the observed current is inversely proportional to the alkanethiol surface coverage. $Ru(NH_3)_6^{3+}$ was selected as an electrochemical probe since it represents a convenient and electrochemically reversible, one-electron redox couple. More importantly, alkanethiol SAMs are stable throughout the electrochemical window in which $Ru(NH_3)_6^{3+}$ redox chemistry occurs.[21]

Potential scans were performed between 0.0 and -0.25 V at a sweep rate of 100 mV/s. Prior to air exposure, the cyclic voltammetry of $Ru(NH_3)_6^{3+}$ at SAM-modified Ag surfaces was recorded. The relevant indicator of SAM surface coverage is the ratio of the peak reduction current for $Ru(NH_3)_6^{3+}$ at the SAM-modified electrode (i_{SAM}) to that measured at a bare Ag surface (i_{Ag}). The quantity (i_{SAM}/i_{Ag}) $\times$ 100% is defined as the normalized percent electrochemically active surface area (%EAS). A bare Ag surface is considered 100% electrochemically active and able to reduce $Ru(NH_3)_6^{3+}$ at the maximum rate. As shown in Table 2, $CH_3(CH_2)_2SH$ SAMs on Ag surfaces are still quite active in electron transfer exhibiting a large %EAS (74.0 $\pm$ 3.3%.) As expected, long chain alkanethiol SAMs block electron transfer more effectively. Cyclic voltammograms for each surface before and after air oxidation are shown and discussed in the Supporting Information for this report.

Surprisingly, air oxidation has little effect on the electron transfer blocking properties of these monolayers, even after 1 week of air exposure, soaking in ethanol for 30 min and copious rinsing with ethanol and water. In fact, the %EAS for an extensively oxidized $CH_3(CH_2)_2SH$ film decreases by a factor

(30) Schlenoff, J. B.; Li, M.; Ly, H. *J. Am. Chem. Soc.* **1995**, *117*, 12528−12536.
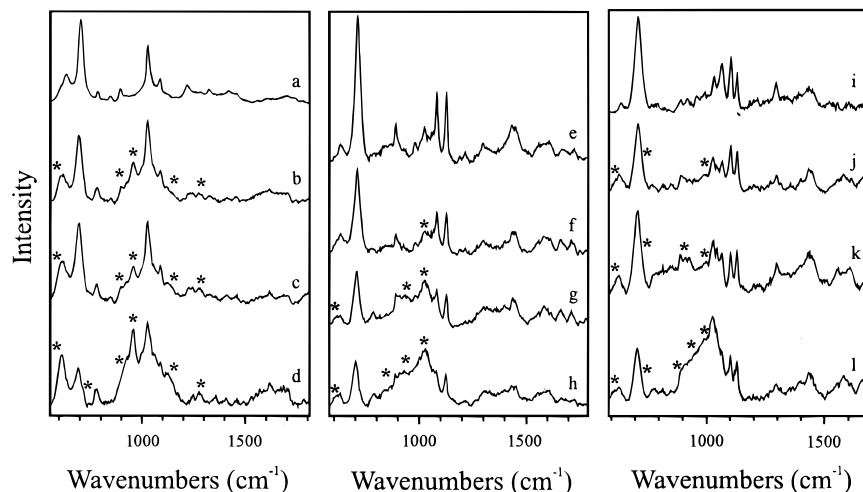
Figure 1. Raman spectra of $CH_3(CH_2)_2SH$ (a–d), $CH_3(CH_2)_{11}SH$ (e–h), and $CH_3(CH_2)_{17}SH$ (i–l) SAMs on Ag after exposure to the ambient environment in the dark for (a), (e), and (i) 0 h, (b), (f), and (j) 2 h, (c), (g), and (k) 6 h, and (d), (h), and (l) 18 h. Spectra for each SAM plotted on same intensity scale. *denotes sulfur oxidation peaks. Integration times are 60 s × 5 collections co-added.
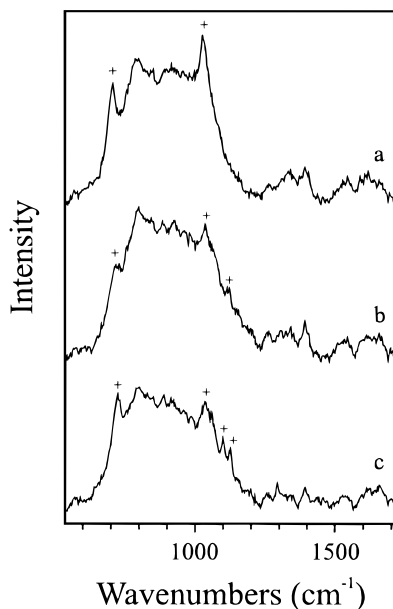
Figure 2. Raman spectra of (a) $CH_3(CH_2)_2SH$, (b) $CH_3(CH_2)_{11}SH$, and (c) $CH_3(CH_2)_{17}SH$ SAMs on Ag after exposure to air for 15 days. + denotes SAM alkyl chain band. Spectra plotted on same intensity scale. Integration times are 60 s × 5 collections co-added.

Figure 3. Raman spectra of $CH_3(CH_2)_2SH$ SAM on Ag after (a) 0 and (b) 20 h air exposure and in 0.1 M NaF at (c) −0.05 V and (d) −1.1 V. Spectra plotted on same intensity scale. *denotes sulfur oxidation peaks. Integration times are 60 s × 5 collections co-added.

of ca. 2. The largely invariant %EAS values indicate that neither the SAM thiolate nor oxidized species desorb from the surface after extensive soaking and rinsing. These results are consistent with the observations noted above from surface Raman spectroscopy of these systems which suggests that the alkane portions of the monolayers remain at the surface. In total, these results suggest that the physical blocking characteristics of well-ordered alkanethiol SAMs are retained even after partial oxidation.

In an effort to increase the solubility of the oxidized species or of alkane chains which may have been cleaved from the sulfur headgroups, similar cyclic voltammetry experiments were undertaken after soaking oxidized SAMs in hexane. In these experiments, alkanethiol-SAMs on Ag were exposed to the ambient environment for 1 week, immersed in neat hexane for 30 min, and then rinsed copiously with hexane and water. As seen in Table 3, the %EAS values for each chain length remain unchanged similar to the behavior observed using ethanol.

The fact that oxidized sulfur species in SAMs are not easily removed by solubilizing solvents contradicts previous re-

Table 2. % Electrochemically Active Surface for SAM-Modified Ag Surfaces after Air Exposure[a]

| SAM | %EAS | | | |
	0 h[a]	3 h	24 h	1 wk
$CH_3(CH_2)_2SH-Ag$[b]	74 ± 3[c]	78 ± 12	67 ± 7	39 ± 13
$CH_3(CH_2)_{11}SH-Ag$	1.4 ± 0.2	1.5 ± 0.3	1.5 ± 0.3	3.2 ± 0.9
$CH_3(CH_2)_{17}SH-Ag$	2.0 ± 0.5	2.6 ± 0.7	2.6 ± 1	2.8 ± 2

[a] After air exposure, SAM-modified Ag electrodes were immersed and stirred in ethanol for 30 min and rinsed with copious amounts of ethanol and H_2O before % EAS determination. All values normalized to bare (unmodified) Ag surfaces. [b] The high % EAS for $CH_3(CH_2)_2SH$ represents efficient electron tunneling through short chain and defects, not exposed surface. [c] Standard deviations result from the analysis of a minimum of three independently prepared SAM films.

ports.[10,11,13] One possible explanation for this discrepancy might be the initial quality of the SAM. As noted above, film quality is extremely sensitive to surface preparation, surface roughness, and film formation conditions. Our results indicate that oxidized

Table 3. % Electrochemically Active Surface after Air Exposure and Hexane Rinse[a]

	%EAS	
SAM	after 1 wk air exposure	after 1 wk air exposure & hexane rinse
CH$_3$(CH$_2$)$_2$SH−Ag	39 ± 13	27 ± 11
CH$_3$(CH$_2$)$_{11}$SH−Ag	3.2 ± 0.9	3.8 ± 2
CH$_3$(CH$_2$)$_{17}$SH−Ag	2.8 ± 2	1.4 ± 0.6

[a] After air exposure, SAM-modified Ag electrodes were immersed and stirred in hexane for 30 min and rinsed with copious amounts of hexane and H$_2$O before % EAS determination. All values normalized to bare (unmodified) Ag surfaces. [b] Standard deviations result from the analysis of a minimum of three independently prepared SAM films.

Table 4. Distribution of Sulfur Species for SAMs on Ag after Air Exposure from XPS

exposure time	% thiolate sulfur[a]	% oxidized sulfur[b]	total % sulfur
	CH$_3$(CH$_2$)$_2$SH		
0	100	0	100
1 h	80.1	8.4	88.5
4 h	72.9	16.0	88.9
24 h	68.5	25.9	93.4
1 wk	49.3	33.4	82.7
	CH$_3$(CH$_2$)$_{11}$SH		
0	100	0	100
1 h	98.5	6.7	105.2
4 h	89.9	16.5	106.4
24 h	63.8	30.6	94.4
1 wk	58.1	47.5	105.6
	CH$_3$(CH$_2$)$_{17}$SH		
0	100	0	100
1 h	92.5	7.7	100.2
4 h	89.5	13.9	103.4
24 h	71.1	31.0	102.1
1 wk	65.8	33.4	99.2

[a] The % thiolate was determined by the ratio of the peak area at 162 eV at time t to the original peak area at 162 eV. [b] The % oxidized sulfur was determined by the ratio of the peak area at 167 eV at time t to the original thiolate peak area at 162 eV.

species formed in well-ordered films resist extraction when exposed to solubilizing solvents.

An alternate explanation is that air oxidation proceeds by a different mechanism than UV-induced oxidation, even though sulfonates are formed in each case. In contrast to the now extensive photopatterning literature, sulfonates formed via air oxidation behave differently than photogenerated sulfonates. One theory might be that in the case of UV-induced oxidation, all of the sulfur is completely oxidized to the corresponding sulfonate, whereas air exposure may produce multiple sulfur oxidation states as suggested in the Raman spectra. It is possible that less oxidized forms of sulfur are more strongly adherent to the metal surface. The above theories are further addressed by control experiments described below.

XPS. XPS was used to confirm that alkanethiol SAMs readily oxidize upon air exposure, determine relative oxidation rates, and ascertain the extent of oxidation. A series of XPS spectra in the sulfur 2p region before and after air exposure are shown in Figure 4 (parts a−e) for CH$_3$(CH$_2$)$_2$SH SAMs, parts f−j for CH$_3$(CH$_2$)$_{11}$SH SAMs, and parts k−o for CH$_3$(CH$_2$)$_{17}$-SH SAMs, respectively. Low X-ray fluxes and short analysis times were used in collecting these spectra in order to minimize sample degradation or X-ray-induced sample reduction. X-ray-induced sample damage is a common problem during XPS analysis of certain materials and can cause spectral changes with X-ray exposure time.[31] Interestingly, the degradation index (a measure of X-ray damage after 500 min exposure to a 1.4 kW X-ray source) is ca. three times greater for sulfone polymers than sulfide polymers[32] confirming the suspected poorer stability of oxidized sulfur species to X-rays.

Immediately after removal from thiol solution, SAM-modified surfaces exhibit a sulfur 2p peak at a binding energy of 162 eV that is characteristic of thiolates on Au and Ag.[33] Following air exposure, the 162 eV thiolate feature decreases in intensity and a new feature at 167 eV emerges. Tarlov et al. observed similar behavior with XPS after exposing CH$_3$(CH$_2$)$_5$SH SAMs on Au to UV irradiation in air; they assigned the 167 eV peak to sulfonate species formed by oxidation.[13] The Raman spectral results discussed above demonstrate that sulfonate and other oxidized sulfur species are formed by dark air exposure suggesting that the 167 eV peak encompasses signals from multiple sulfur oxidation states.

Time-dependent changes in the XPS spectra indicate that the oxidation rate varies as a function of chain length. The rates of oxidation were evaluated for each SAM by measuring the combined areas of the thiolate and sulfonate peaks after 1 h, 4 h, 24 h, and 1 week of air exposure. Values of the thiolate and sulfonate sulfur 2p peak areas normalized to the initial thiolate peak area are given in Table 4. Clearly, CH$_3$(CH$_2$)$_2$SH SAMs oxidize to a greater extent than the long chain monolayers. Furthermore, the oxidation rates observed with XPS are consistent with those observed using Raman spectroscopy.

If the oxidized thiol remains at the surface, the percentage of thiolate and oxidized sulfur species should combine to 100% assuming that the X-ray cross-sections are approximately equivalent for these two species. To within ca. 5%, such behavior is observed for CH$_3$(CH$_2$)$_{11}$SH and CH$_3$(CH$_2$)$_{17}$SH SAMs on Ag. However, for CH$_3$(CH$_2$)$_2$SH SAMs, ca. 10−20% of the sulfur signal is lost after oxidation. Control experiments in which unoxidized CH$_3$(CH$_2$)$_2$SH films on Ag were exposed to a similar flux of X-rays for 15 min indicate an ca. 5% decrease in sulfur signal compared to an ca. 13% decrease in total sulfur signal (both 162 and 167 eV peaks) for partially oxidized films (3 h air exposure). These results suggest that the sulfur signal decrease in oxidized films is due to X-ray degradation of the oxidized sulfur species. This degradation is most easily seen for CH$_3$(CH$_2$)$_2$SH SAMs because of the extent to which they oxidize relative to the longer chain SAMs in the time frame of the experiment.

SAMs on Au. Raman Spectroscopy. Air exposure experiments on ordered *n*-alkanethiol (CH$_3$(CH$_2$)$_n$SH, n = 2, 11, 17) SAMs on Au before and after exposure to the ambient air environment were performed and compared to the behavior observed on Ag. The sensitivity of Raman spectroscopy for SAMs on Au is greatly reduced relative to Ag for several reasons. First, the maximum surface enhancement for Au surfaces is achieved with near-IR excitation.[35] However, the surface enhancement for Au with 720 nm excitation is much less than that for Ag with 514.5 nm excitation. In addition, monochromator throughput and CCD quantum efficiency at 720 nm are significantly reduced. Therefore, to improve signal levels in these experiments, Au surfaces were roughened slightly to provide weak surface enhancement.

(31) Graham, R. L.; Bain, C. D.; Biebuyck, H. A.; Laibinis, P. E.; Whitesides, G. M. *J. Phys. Chem.* **1993**, *97*, 9456−9464.

(32) Beamson, G.; Briggs, D. *High-Resolution XPS of Organic Polymers*; John Wiley & Sons: New York, 1992; pp 258−260.

(33) Laibinis, P. E.; Whitesides, G. M.; Allara, D. L.; Tao, Y.-T.; Parikh, A. N.; Nuzzo, R. G. *J. Am. Chem. Soc.* **1991**, *113*, 7152−7167.

(34) Mrksich, M.; Grunwell, J. R.; Whitesides, G. M. *J. Am. Chem. Soc.* **1995**, *117*, 12009−12010.

(35) Chase, D. B.; Parkinson, B. A. *Appl. Spec.* **1988**, *42*, 1186−1187.
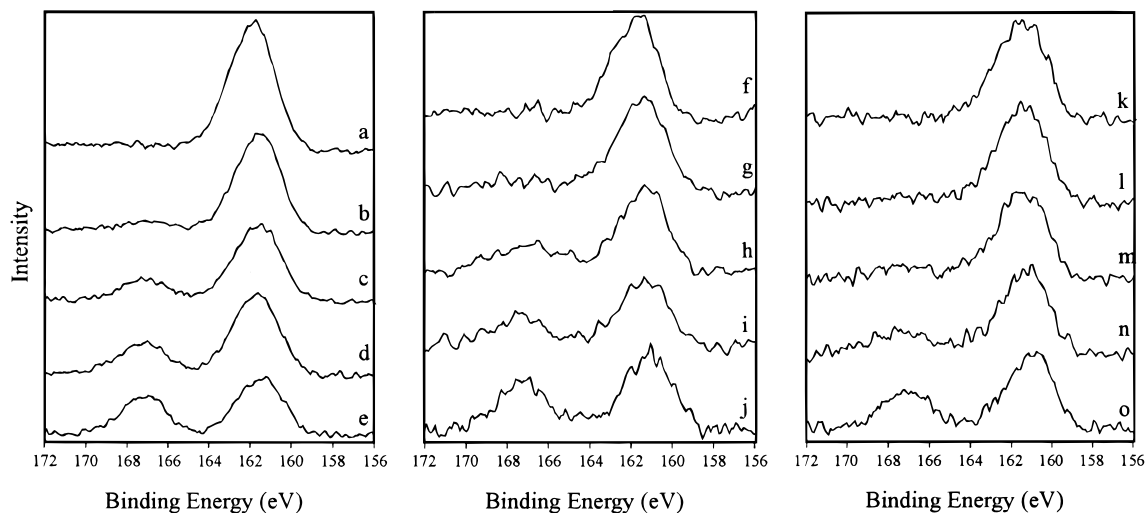
Figure 4. XPS spectra of S 2p region acquired from $CH_3(CH_2)_2SH$ (a–e), $CH_3(CH_2)_{11}SH$ (f–j), and $CH_3(CH_2)_{17}SH$ (k–o) SAMs on Ag after exposure to ambient environment for (a), (f), and (k) 0 h, (b), (g), and (l) 1 h, (c), (h), and (m) 4 h, (d), (i), and (n) 24 h, and (e), (j), and (o) 1 week. Spectra for each SAM plotted on same intensity scale.
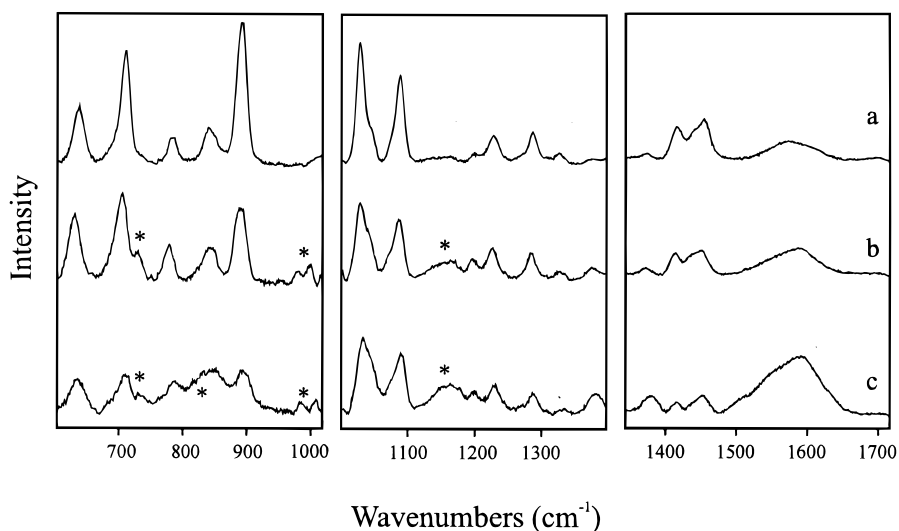
Figure 5. Raman spectra of $CH_3(CH_2)_2SH$ SAM on Au after exposure to the ambient environment for (a) 0 h, (b) 6 h, and (c) 20 h. Spectra plotted on same intensity scale. *denotes sulfur oxidation peaks. Integration times are for 10 s × 90 collections co-added.

SAMs on these Au surfaces are well-ordered and essentially completely blocking as indicated by capacitance values of 7.5 ± 3.3, 2.7 ± 1.3, and 2.2 ± 0.7 $\mu F/cm^2$ for $CH_3(CH_2)_2SH$, $CH_3(CH_2)_{11}SH$, and $CH_3(CH_2)_{17}SH$ films, respectively. These values are in good agreement with previously reported values for well-ordered SAMs on freshly evaporated Au surfaces.[26–28] These measurements indicate that slight surface roughening does not have a significant effect on film order.

As a result of increased spectrograph dispersion at 720 nm, three Raman spectral regions were collected for each film in order to obtain vibrational information from 600 to 1700 cm^{-1}. Although three measurements are more time-intensive, spectral resolution is greatly improved, further clarifying the oxidation behavior.

Surface Raman spectra for $CH_3(CH_2)_2SH$, $CH_3(CH_2)_{11}SH$, and $CH_3(CH_2)_{17}SH$ SAMs on slightly roughened Au surfaces are shown in Figures 5–7, respectively. The top spectrum in each of these figures is from a freshly prepared SAM in N_2 prior to air exposure. Upon air exposure, evidence for oxidation similar to that observed on Ag is detected for SAMs on Au. Specifically, the spectra after 6 h air exposure show new peaks at ca. 615, 850, 917, 980, and 1010 cm^{-1} corresponding to

sulfonate, sulfonite, sulfate, and sulfite species, respectively.[29] Further evidence for sulfonate and sulfonite formation is observed in the $\nu(C-C)$ region. In particular, the broad peak at 1150 cm^{-1} is another indication of sulfur oxidation. This peak is most likely due to the overlap of $\nu(R-SO_3^-)$ and $\nu(R-OSO_3^{2-})$ bands at 1127 and 1195 cm^{-1}, respectively.[36] The intensities of these bands increase with air exposure time, similar to the behavior observed on Ag.

Bands at 1390 and 1590 cm^{-1} suggestive of graphitic carbon are also observed upon oxidation and increase significantly with air exposure. *Such an effect was not observed for SAMs on Ag* and may be indicative of considerable monolayer decomposition on Au. Specifically, the significant increase in the intensity of the 1590 cm^{-1} band with oxidation suggests a different mechanism for oxidation on Au. This point is discussed further below.

The dependence of oxidation rate on SAM chain length on Au is slightly different from that observed on Ag. The least stable SAM on Au appears to be $CH_3(CH_2)_{11}SH$. After only 6

(36) Dollish, F. R.; Fateley, W. G.; Bentley, F. F. *Characteristic Raman Frequencies of Organic Compounds*; John Wiley & Sons: New York, 1974; Chapter 5, p 46.
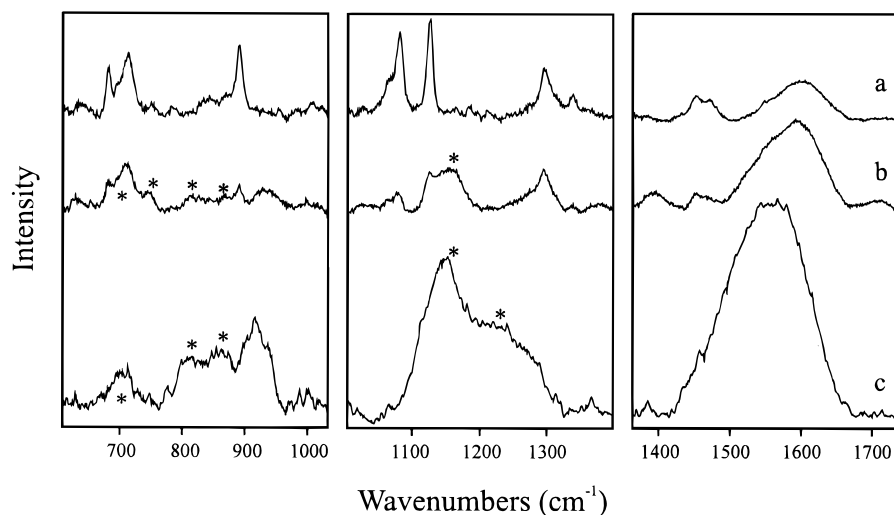
Figure 6. Raman spectra of $CH_3(CH_2)_{11}SH$ SAM on Au after exposure to the ambient environment for (a) 0 h, (b) 6 h, and (c) 20 h. Spectra plotted on same intensity scale. *denotes sulfur oxidation peaks. Integration times are for 10 s × 90 collections co-added.
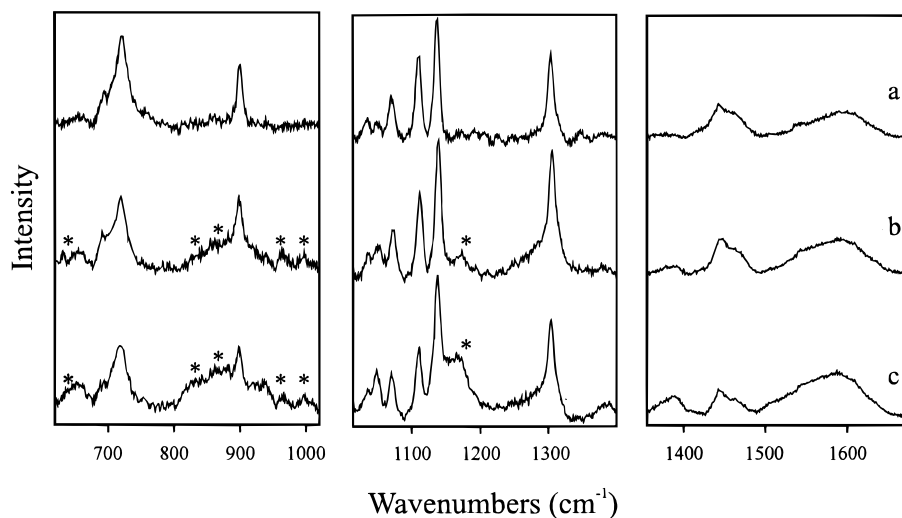
Figure 7. Raman spectra of $CH_3(CH_2)_{17}SH$ SAM on Au after exposure to the ambient environment for (a) 0 h, (b) 6 h, and (c) 20 h. Spectra plotted on same intensity scale. *denotes sulfur oxidation peaks. Integration times are 10 s × 90 collections co-added.

h of air exposure, significant sulfur oxidation occurs. In addition, the intensities of several monolayer modes decrease including the $\nu(C-S)_T$ at 705 cm^{-1}, the CH_3 rock at 890 cm^{-1}, the $\nu(C-C)$ at 1064, 1106, and 1128 cm^{-1}, the CH_2 wag at 1300 cm^{-1}, the CH_2 twist at 1430 cm^{-1}, and the CH_2 scissor at 1452 cm^{-1}. These changes are even more pronounced after 20 h of air exposure, suggesting either hydrocarbon chain degradation or considerable disorder induced by oxidation. The SAM most resistant to oxidation on Au is $CH_3(CH_2)_{17}SH$. However, $CH_3(CH_2)_{17}SH$ also shows signs of oxidation after the surface is exposed to air for 6 h, similar to its behavior on Ag.

Differences between the oxidation behavior on Au and Ag are significant. First, the overall dramatic decrease in SAM band intensity on Au is not observed on Ag. Furthermore, the emergence of the 1590 cm^{-1} mode is only observed on Au. *These results imply different mechanisms for SAM oxidation on these two metals.* On Au, the initial decrease in SAM band intensity suggests either that oxidation of the sulfur headgroup requires removal of the hydrocarbon chains to allow easier access by the oxidant species[16] or that the Au surface is oxidized.[19] If the latter process occurs, a surface with greater activity toward C–S bond cleavage may result, thereby explaining the growth of the band at 1590 cm^{-1} as oxidation proceeds.

XPS. XPS was used to confirm air oxidation of SAMs on Au. XPS spectra from $CH_3(CH_2)_2SH$, $CH_3(CH_2)_{11}SH$, and $CH_3(CH_2)_{17}SH$ SAMs on Au are shown in Figure 8 (parts a–d, e–i, and j–n, respectively). The poorer S/N of the spectra on Au relative to those on Ag is a result of greater inelastic electron scattering processes at Au. Relative areas of the thiolate and sulfonate sulfur 2p peaks are given in Table 5. Oxidation similar to that on Ag occurs for SAMs on Au, albeit with certain significant differences. The oxidation rate is clearly a function of chain length; short chain SAMs (e.g., $CH_3(CH_2)_2SH$) oxidize more quickly than long chain $CH_3(CH_2)_{11}SH$ or $CH_3(CH_2)_{17}$-SH SAMs on Au.

The XPS results confirm that SAMs on Au are less stable than those on Ag. A rapid and complete loss of intensity of the thiolate sulfur 2p peak at 162 eV occurs for all chain lengths upon air exposure. On Ag after 1 week of air exposure, the intensity of the thiolate sulfur 2p peak is still greater than that of the oxidized sulfur peak at 167 eV. In contrast, the peak at 167 eV on Au disappears for both $CH_3(CH_2)_2SH$ and $CH_3(CH_2)_{11}$-SH SAMs on Au after only 24 h of air exposure and for $CH_3(CH_2)_{17}SH$ on Au after 1 week. Furthermore, the combined peak areas for these two sulfur 2p bands *do not sum to 100%*

Table 5. Distribution of Sulfur Species for SAMs on Au after Air Exposure from XPS

exposure time	% thiolate sulfur[a]	% oxidized sulfur[b]	total % sulfur
	$CH_3(CH_2)_2SH$		
0	100	0	100
1 h	15.0	55.2	70.2
4 h	8.5	61.2	69.7
24 h	NM[c]	88.8	88.8
	$CH_3(CH_2)_{11}SH$		
0	100	0	100
1 h	63.1	15.2	78.3
4 h	43.6	31.0	74.6
24 h	NM	63.7	63.7
1 wk	NM	72.2	72.2
	$CH_3(CH_2)_{17}SH$		
0	100	0	100
1 h	72.0	NM	72.0
4 h	65.1	NM	65.1
24 h	42.1	55.5	97.6
1 wk	NM	80.5	80.5

[a] The % thiolate was determined by the ratio of the peak area at 162 eV at time t to the original peak area at 162 eV. [b] The % oxidized sulfur was determined by the ratio of the peak area at 167 eV at time t to the original thiolate peak area at 162 eV. [c] NM denotes peak areas were not measurable.

for any of the three SAMs on Au, clearly indicating partial loss of sulfur from the surface upon oxidation, perhaps as gaseous SO_3.

Partially oxidized $CH_3(CH_2)_2SH$ SAMs on Au (3 h in air) exposed to a similar flux of X-rays for 15 min exhibit an ca. 14% decrease in total sulfur signal (combined 162 and 167 eV peaks). Control experiments on unoxidized $CH_3(CH_2)_2SH$ SAMs exhibit a decrease of only ca. 5% of the 162 eV peak, similar to the behavior observed at Ag. These results suggest that sulfonates are ca. three times more likely to degrade upon X-ray exposure than thiolates. SAMs on Au are oxidized to a greater extent; therefore, a slightly greater loss of sulfur is observed from Au than Ag. Oxidized $CH_3(CH_2)_2SH$ SAMs on Au left in ultrahigh vacuum for extended times (ca. 12 h) without X-ray exposure manifest *no* peak area diminution.

Of additional significance in these XPS data is the indication of multiple oxidation states of the sulfur headgroup. This chemistry is most clearly demonstrated in the spectra from $CH_3(CH_2)_2SH$ after long air exposure times in which shoulders at ca. 166.5 and 169 eV are observed on the central band at ca. 167.5 eV. Similar broadening of the 167 eV band is observed for $CH_3(CH_2)_{11}SH$ and $CH_3(CH_2)_{17}SH$ for long oxidation times. This behavior is consistent with the Raman spectral evidence for multiple states of oxidation discussed above.

Cyclic Voltammetry. Cyclic voltammetry of $Ru(NH_3)_6^{3+}$ was also performed to assess the stability of sulfonates in SAMs on Au. As shown in Table 6, oxidized SAMs on Au after 24 h and 1 week of air exposure are not easily removed, even when stirred in ethanol for 30 min and rinsed with copious amounts of ethanol and water. This observation is similar to that made for alkanethiols on Ag. Furthermore, the blocking properties of the film are maintained, despite oxidation. These results, in combination with those from the Raman spectroscopy and XPS experiments, suggest that although extensive degradation of the thiolate headgroup occurs via oxidation, the partially decomposed hydrocarbon chains remain at the surface and prevent electron transfer to $Ru(NH_3)_6^{3+}$.

Control Experiments. In an effort to gain a better understanding of alkanethiol oxidation, several control experiments were undertaken. Surface Raman spectra for $CH_3(CH_2)_2SH$ SAMs on Ag were collected after exposure to different

Table 6. % Electrochemically Active Surface for SAM-Modified Au Surfaces after Air Exposure[a]

SAM	0 h	24 h	1 wk
$CH_3(CH_2)_2SH-Au$[b]	66 ± 12[c]	69 ± 15	86 ± 2
$CH_3(CH_2)_2SH-Au$	9.4 ± 8	8.9 ± 6	9.7 ± 2
$CH_3(CH_2)_2SH-Au$	3.2 ± 1	2.1 ± 1	1.9 ± 0.5

[a] After air exposure, SAM-modified Au electrodes were immersed and stirred in ethanol for 30 min and rinsed with copious amounts of ethanol and H_2O before % EAS determination. All values normalized to bare (unmodified) Au surfaces. [b] The high % EAS for $CH_3(CH_2)_2SH$ represents efficient electron tunneling through short chain and defects, not exposed surface. [c] Standard deviations result from the analysis of a minimum of three independently prepared films.

controlled atmosphere environments including pure N_2, pure O_2, compressed air, ambient environments in another lab and a private residence, and an O_3-enriched air environment. $CH_3(CH_2)_2SH$ SAMs were selected for these experiments over longer chain lengths because of its greater reactivity toward oxidation.

As shown in Figure 9a, no oxidation bands appear if the SAM is exposed to a pure N_2 environment for 24 h, the maximum time investigated. Such behavior is expected. Surprisingly, however, exposure of the $CH_3(CH_2)_2SH$ SAM to pure O_2 for 24 h results in very minimal oxidation (Figure 9b) as evidenced by the slightly broadened background beneath the 890 cm^{-1} SAM band, a shoulder on the $\nu(C-C)$ mode at 1026 cm^{-1}, and new peaks at 1204, 1256, 1290, and 1389 cm^{-1}. Clearly, massive film degradation due to oxidation, similar to that observed in the ambient laboratory air after only 1−2 h of exposure, does not occur. Similar observations were made with a water-saturated O_2 environment suggesting that neither O_2 nor water is the primary oxidant in ambient laboratory air. As shown in Figure 9c, exposure to compressed air results in a similar outcome; no significant oxidation is observed, even if the air is saturated with water vapor (data not shown).

At this point in our studies, the possible components of our ambient laboratory air were meticulously assessed. Ag surfaces modified with $CH_3(CH_2)_2SH$ SAMs were exposed to the ambient environment in different rooms in our building, another building on campus, and at a private residence. Transfer of these surfaces took place at night in a vessel containing N_2, and at no time were the SAMs exposed to light. The Raman spectra of these surfaces after 12 h of air exposure in another building and a private residence are shown in Figure 9 (parts d and e, respectively). As was observed in our laboratory, the SAM exposed to the ambient air in different rooms in our building and another building on campus (Figure 9d) oxidized extensively as indicated by oxidation bands at 615, 875, 975, 1040, and 1147 cm^{-1}. Only slight oxidation was observed for the $CH_3(CH_2)_2SH$ film stored overnight at a private residence as shown in Figure 9e, indicating some difference between the ambient air in these two environments.[37]

Residual gas analysis of our laboratory air was performed with mass spectrometry. Air was leaked into a UHV system such that the base pressure increased to 5×10^{-7} Torr, and the mass spectral response was monitored at m/z 48 as a function of time. As shown in Figure 10, O_3 is clearly found to be a

(37) After a lengthy discussion with building engineers at our institution, it became apparent that the air handlers at the University of Arizona bring in 100% outside air for cooling (and heating when necessary) for all university buildings; no percentage of building air is recycled. Particularly important for laboratory buildings is that significant air flow is maintained, to continuously replace laboratory air which exits the building through fume hoods. Herein lies the variance between the university and private residence environments. In the private residence, the air flow is considerably reduced.
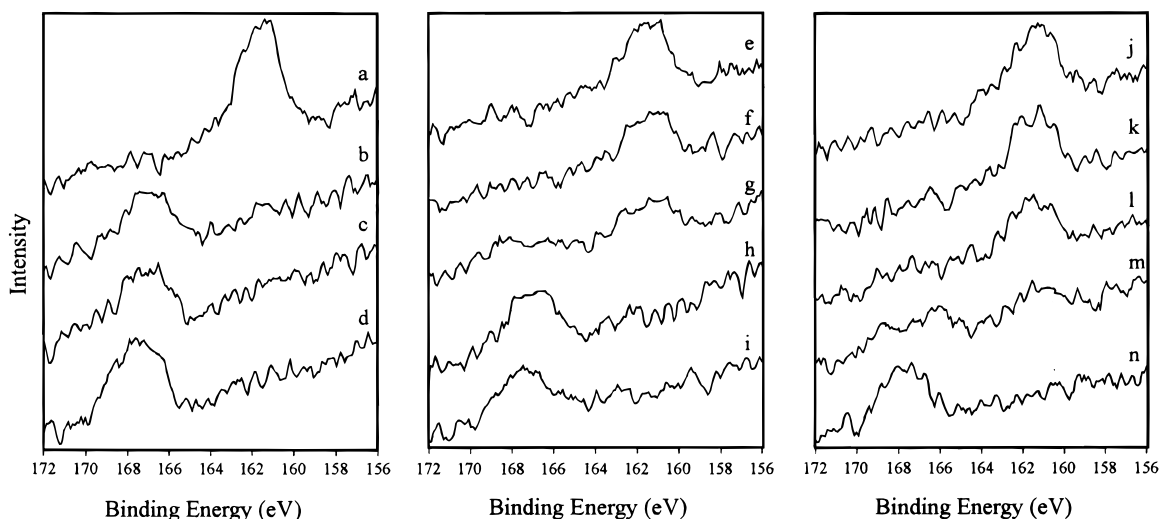
Figure 8. XPS spectra of S 2p region acquired from $CH_3(CH_2)_2SH$ (a−d), $CH_3(CH_2)_{11}SH$ (e−i), and $CH_3(CH_2)_{17}SH$ (j−n) SAMs on Au after exposure to ambient environment for (a), (e), and (j) 0 h, (b), (f), and (k) 1 h, (c), (g), and (l) 4 h, (d), (h), and (m) 24 h, and (i) and (n) 1 week. Spectra for each SAM plotted on same intensity scale.
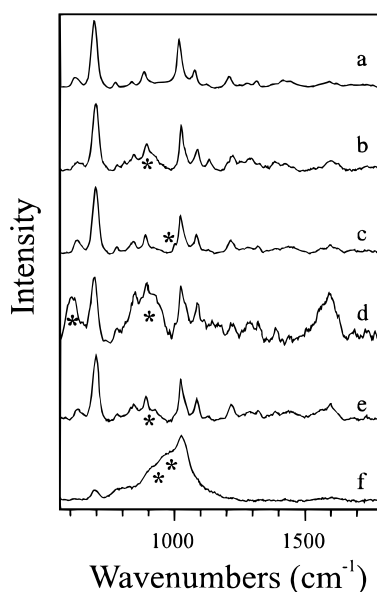
Figure 9. Raman spectra of $CH_3(CH_2)_2SH$ SAM on Ag after exposure to (a) 100% N_2 for 24 h, (b) 100% O_2 for 24 h, (c) compressed air for 24 h, (d) ambient environment in another building on campus, (e) ambient environment at private residence for 12 h, and (f) O_3/compressed air-mixture for 30 s. Integrations times are 120 s.

small component of our laboratory environment; this experiment was repeated in another laboratory and O_3 was also detected.

O_3 levels in Tucson and throughout the southwestern United States, where sunlight is abundant, are known to be higher than those in other parts of the country. (O_3 formation is accelerated by UV light from the sun.)[38] The hypothesis that O_3 is the primary oxidant in air is consistent with the work of Linton and Worley who demonstrated that gold surfaces exposed to

---

(38) For example, during the month of July, 1996, the average hourly O_3 level as monitored by the U.S. Environmental Protection Agency was 46% higher than O_3 measured in cental Iowa (0.041 versus 0.028 ppm). O_3 levels are also greater in cities such as Tucson which are surrounded by mountains which trap air pollution. For that same month, the average hourly O_3 level in Palm Springs, CA, was measured at 0.063 ppm. Naturally, O_3 levels in a building for which a large percentage of air is continually recycled will be higher than those having lessened circulation (e.g., private residence) or partially recycled circulation. (Ozone values obtained from the U.S. Environmental Protection Agency at *www.epa.gov* through Tom Coffin at the Pima County Department of Environmental Quality, Tucson, AZ).
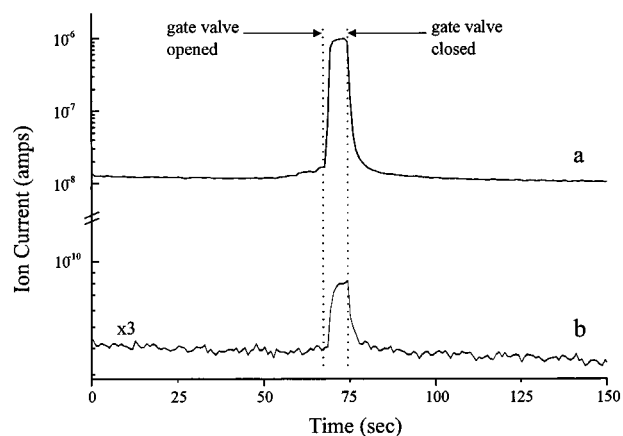
Figure 10. Residual gas analysis by quadrupole mass spectrometer monitoring (a) O_2 (*m/z* 32) and (b) O_3 (*m/z* 48).

UV light in air are purged of sulfur impurities via the oxidation of chemisorbed sulfur to sulfonates by ozone and atomic oxygen formed by the UV light.[39]

To further test whether O_3 might be accelerating thiolate oxidation, a mixture of O_3 and compressed air was generated in a glovebag. As shown in Figure 9f, exposure of the $CH_3(CH_2)_2SH$ SAM to this environment for only 30 s results in rapid and almost complete oxidation. Similar behavior occurs for $CH_3(CH_2)_{17}SH$ SAMs on Ag, as shown in Figure 11, although their rate of oxidation is much slower. Moreover, a progression of oxidation modes is observed as a function of O_3 exposure for $CH_3(CH_2)_{17}SH$ SAMs as evidenced by increases in the sulfonate oxidation bands at 615, 725, 917, and 975 cm^{-1}. This behavior is consistent with slower penetration of O_3 through the longer SAM.

The SAM bands decrease in intensity with O_3 exposure with a concomitant increase of bands at 1390 and 1590 cm^{-1}. This behavior, not previously observed on Ag even after air exposure for 1 week, suggests C−S bond cleavage and possibly alkane chain degradation at sufficiently high oxidant concentrations. This bond cleavage could occur directly by oxidation[16] or through surface oxidation[19] to produce a catalytic surface for this cleavage reaction. Moreover, sulfonite oxidation modes

---

(39) Linton, R. W.; Worley, C. G. *J. Vac. Sci. Technol. A* **1995**, *13(4)*, 2281−2284.
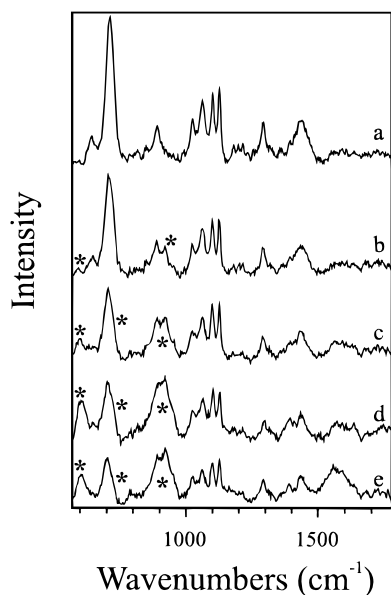
Figure 11. Raman spectra of $CH_3(CH_2)_{17}SH$ SAM on Ag (a) before and after exposure to O_3/compressed air-mixture for (b) 5 min, (c) 15 min, (d) 40 min, and (e) 1 h. Spectra plotted on same intensity scale. *denotes sulfur oxidation peaks. Integration times are 120 s.

at 1034, 1040, 1127, and 1195 cm^{-1} are never observed, indicating that intermediate oxidation states of sulfur are extremely unstable in this highly oxidizing environment.

$CH_3(CH_2)_2SH$ and $CH_3(CH_2)_{17}SH$ SAMs on Au were also exposed to the O_3-compressed air environment. Raman spectra for a $CH_3(CH_2)_{17}SH$ SAM on Au before and after O_3 exposure are shown in Figure 12. Oxidized sulfur modes at 615, 850, 917, 975, 1010, and 1150 suggest considerable oxidation. Furthermore, the SAM bands decrease by ca. 70% and the 1390 and 1590 cm^{-1} modes become quite prominent suggesting significant alkane chain degradation. These observations are further confirmation of the conclusion presented above that SAMs on Au are more reactive toward oxidation than SAMs on Ag.

Finally, the stability of thiophenol (TP) SAMs on Ag was briefly investigated. Garrell and co-workers have reported that monolayers formed from aromatic thiols on Au are significantly more robust and less prone to air and electrochemical oxidation than alkanethiol SAMs.[11,40,41] Raman spectra for TP SAMs before and after O_3 exposure are shown in Figure 13. The ca. 90% decreases in intensity of the ring breathing and bending modes at 997, 1019, and 1070 cm^{-1} suggest O_3 exposure causes cleavage of the C–S bond of TP either directly[16] or through surface oxidation.[19] Broadening of the band at ca. 1590 cm^{-1} suggests the appearance of carbon as this process proceeds. These results indicate that aromatic thiols on Ag are not totally immune to oxidation in environments containing high levels of O_3.

Based on the above experiments, O_3 appears to be the primary oxidant in the ambient laboratory environment that causes rapid air oxidation of alkanethiol SAMs on Ag and Au. This hypothesis may explain the current discrepancy regarding rapid air oxidation of SAMs in the community. Studies performed in laboratory environments in which O_3 levels are low will result in less SAM oxidation. The O_3 concentration in laboratory air in a given location is a function of several factors including

outdoor O_3 levels, fresh air circulation, and air flow. In buildings in which partial air recirculation is a regular mechanism by which laboratory air is provided, the oxidation rate of SAMs will be less for a given O_3 level in the outside air.

Oxidation Mechanism. There have been few investigations of the reaction of O_3 with organosulfur compounds.[42-44] The first notable study involved the infrared spectroscopic analysis of the reaction of ground-state oxygen atoms, generated by visible photolysis of O_3, with dimethyl sulfide and CH_3SH in solid argon matrixes.[42] Oxygen atoms were shown to react in a stepwise mechanism with dimethyl sulfide in argon matrixes to produce dimethyl sulfoxide and dimethyl sulfone with no apparent activation barrier *even at 10 K*. Co-deposition of CH_3-SH and O_3 produced oxidation bands which were assigned to –C–O–S– and –C–S–O– linkages, suggesting multiple oxidation products. Photolysis of these matrixes increased product yield. When these reactions were carried out in the gas phase, HSO• species were produced resulting in C–S bond cleavage.

The results of this study support our conclusions regarding the oxidation of alkanethiol SAMs by O_3. The ease with which CH_3SH is oxidized at 10 K supports the high reactivity of O_3 with sulfur at room temperature. Mechanisms for UV-induced oxidation are proposed to occur by the interaction of sulfur with singlet oxygen,[18] a product of O_3 decomposition. We propose a similar mechanism for air-induced oxidation without UV-surface irradiation.

XPS and Raman spectroscopy of oxidized SAMs suggest that these films on Ag are more stable than on Au. This enhanced stability on Ag is proposed to be due to the greater strength of the Ag–S bond. The Ag–S bond is expected to be more ionic than the Au–S bond based on the electronegativity differences between S and these two metals.[25] Significantly, C–S bond cleavage is observed to a greater extent on Au than on Ag as evidenced by a decrease in intensity of the bands attributed to the monolayer and the appearance of amorphous carbon modes. Only after O_3 levels are dramatically increased is similar behavior observed for SAMs on Ag.

This hypothesis is further supported by the changes observed in the XPS carbon 1s data from SAM-modified Ag and Au surfaces. Carbon 1s peak areas normalized to either the Ag $3d_{5/2}$ or Au $4d_{5/2}$ peak as a function of air exposure time are given in Table 7. Pronounced *loss* of carbon 1s intensity occurs for $CH_3(CH_2)_{11}SH$ and $CH_3(CH_2)_{17}SH$ SAMs on Au; however, for all three SAMs on Ag and for $CH_3(CH_2)_2SH$ on Au, the carbon 1s intensity remains essentially constant with air exposure time. These data imply significant loss of the alkane portions of oxidized longer chain SAMs on Au in the UHV environment, consistent with the loss of sulfur XPS signal for the same SAMs on Au as noted above. Such losses in UHV could occur through a mechanism involving C–S bond cleavage resulting in volatile hydrocarbons and possibly SO_3. In solution or at atmospheric pressure, hydrocarbon species created in such fashion would be expected to adhere to the Au electrode surface as poisons. In fact, the blocking characteristics of oxidized $CH_3(CH_2)_{11}SH$ and $CH_3(CH_2)_{17}SH$ SAMs on Au toward electron transfer (see Supporting Information) is consistent with this picture.

(40) Garrell, R. L.; Chadwick, J. E. *Colloids Surf. A* **1994**, *93*, 59–72.

(41) Chadwick, J. E.; Myles, D. C.; Garrell, R. L. *J. Am. Chem. Soc.* **1993**, *115*, 10364–10365.

(42) Tevault, D. E.; Mowery, R. L.; Smardzewski, R. R. *J. Chem. Phys.* **1981**, *74*, 4480–4487.

(43) Le Sauze, N.; Laplanche, A.; Martin, G.; Paillard, H. *Ozone: Sci. Eng.* **1991**, *13*, 331–347.

(44) Jaeger, K.; Weller, R.; Schrems, O. *Proc. SPIE-Int. Soc. Opt. Eng.* **1992**, *1575*, 333–334.
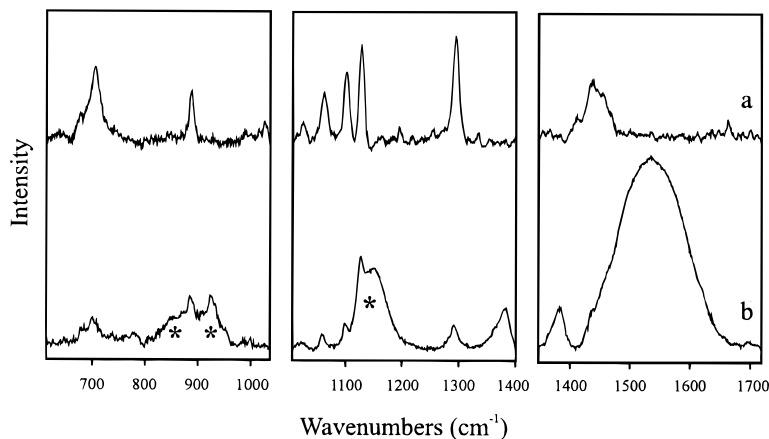
Figure 12. Raman spectra of $CH_3(CH_2)_{17}SH$ SAM on Au (a) before and (b) after exposure to O_3/compressed air-mixture for 30 min. Spectra plotted on same intensity scale. *denotes sulfur oxidation peaks. Integration times are 10 s × 60 collections co-added.
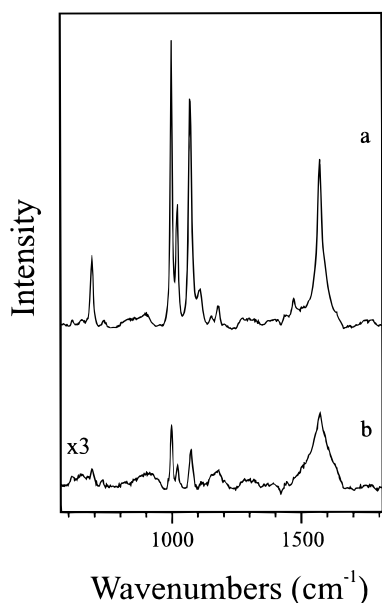
Figure 13. Raman spectra of thiophenol SAM on Ag (a) before and (b) after exposure to O_3/compressed air-mixture for 30 min. Integration times are 120 s.

Conclusions

The results presented here clearly support oxidation of alkanethiol self-assembled monolayers on Ag and Au upon air exposure in the absence of light. The extent of this oxidation is small enough after one week of dark air exposure that these SAMs still generally retain their integrity with respect to electron transfer blocking properties. Therefore, the potential utility of SAMs for many applications may not be sacrificed if they are exposed to air for only brief periods or stored in solution where oxidation is considerably slower.[45]

Many factors affect alkanethiol oxidation, including chain length, initial film quality, nature of the metal substrate, and atmospheric O_3 levels. Raman spectroscopy and XPS indicate that the oxidation rate varies strongly with alkyl chain length. Long chain length SAMs oxidize much more slowly because of the inability of the active oxidant species to penetrate the closely packed alkyl chain structure. Short chain SAMs oxidize at faster rates as a result of shorter distances between the outside of the SAM and the sulfur headgroup and the greater number of defects. Similarly, poorly formed films containing large

(45) Deschaines, T. O.; Carron, K. T. *Appl. Spectrosc.* **1997**, *51*, 1355–1359.

Table 7. Normalized XPS C 1s Peak Areas[a] as a Function of Air Exposure

SAM	exposure time	Ag	Au
$CH_3(CH_2)_2SH$	0 h	0.15	0.36
	1 h	0.15	0.32
	4 h	0.14	0.34
	24 h	0.15	0.38
	75 h	N.D.[b]	0.38
	1 wk	0.18	N.D.[b]
$CH_3(CH_2)_{11}SH$	0 h	0.26	0.27
	1 h	0.30	0.20
	4 h	0.26	0.17
	24 h	0.24	0.13
	1 wk	0.23	0.13
$CH_3(CH_2)_{17}SH$	0 h	0.46	0.55
	1 h	0.43	0.49
	4 h	0.41	0.46
	24 h	0.41	0.44
	1 wk	0.43	0.41

[a] Carbon 1s peak areas (284 eV) were normalized to the peak areas of either Ag $3d_{5/2}$ (368 eV) or Au $4s_{5/2}$ (87 eV) for SAM-modified Ag or Au, respectively. [b] N.D. denotes data not available.

numbers of defects are less stable. *In contrast to previous literature reports, SAMs formed on Au are significantly less stable than those on Ag.* Finally, O_3 has been identified as the likely oxidant in air that causes rapid alkanethiol oxidation. Conflicting reports on the stability of SAMs in air are probably due to a combination of the above factors; however, the concentration of O_3 in laboratory air (related to atmospheric O_3 levels and building air flow and circulation) is probably the defining factor.

Supporting Information Available: Cyclic voltammograms of $CH_3(CH_2)_2SH$, $CH_3(CH_2)_{11}SH$, and $CH_3(CH_2)_{17}SH$ SAMs on Ag and Au after soaking/rinsing in ethanol (neat) and water before and after 1 week of air exposure (5 pages, print/PDF). See any current masthead page for ordering information and Web access instructions.

JA974301T